Investigation of a household-scale open sorption energy storage system based on the Zeolite 13X/water reacting pair

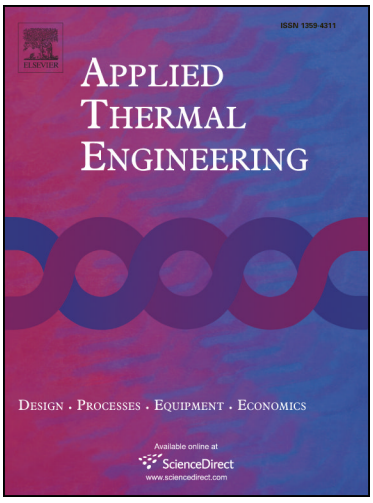

Investigation of a household-scale open sorption energy storage system based on the Zeolite 13X/water reacting pair

R. van Alebeek, L. Scapino, M.A.J.M. Beving, M. Gaeini, C.C.M. Rindt, H.A. Zondag

PII: S1359-4311(17)37043-6
DOI: https://doi.org/10.1016/j.applthermaleng.2018.04.092
Reference: ATE 12089

To appear in: *Applied Thermal Engineering*

Received Date: 3 November 2017
Revised Date: 21 March 2018
Accepted Date: 19 April 2018

Please cite this article as: R. van Alebeek, L. Scapino, M.A.J.M. Beving, M. Gaeini, C.C.M. Rindt, H.A. Zondag, Investigation of a household-scale open sorption energy storage system based on the Zeolite 13X/water reacting pair, *Applied Thermal Engineering* (2018), doi: https://doi.org/10.1016/j.applthermaleng.2018.04.092

Investigation of a household-scale open sorption energy storage system based on the Zeolite 13X/water reacting pair

R. van Alebeek [1], L. Scapino[1,2], M.A.J.M. Beving [1], M. Gaeini [1], C.C.M. Rindt [1,], H.A. Zondag [1,3]*

[1] Eindhoven University of Technology, Department of Mechanical Engineering, 5600 MB Eindhoven, The Netherlands
[2] VITO NV, Energy Technology unit, Thermal Systems group, Boeretang 200, BE-2400 Mol, Belgium
[3] Energy Research Centre of the Netherlands (ECN), 1755 ZG Petten, The Netherlands
* Corresponding author. Email: C.C.M.Rindt@tue.nl

Abstract

Sorption thermal energy storage is a promising concept for seasonal heat storage. Advantages of sorption heat storage are high energy storage density (compared to sensible and phase change heat storage) and negligible energy losses during storage over long time periods. In order to investigate the potential of sorption thermal energy storage, a high power open sorption heat storage system has been designed and built for household space heating applications. In this paper, the characteristics of the open zeolite 13X/water sorption energy storage system will be presented. The setup consists of four segments with a total capacity of 250 liters of zeolite. A segmented reactor has been designed to reduce the pressure drop over the system, which results in less required fan power. This configuration also decreases the response time and makes the system scalable. Dehydration of the reactor is performed by supplying hot air to the zeolite bed. Hydration is performed by supplying humidified air to the bed. In all the segments, the pressure drop, temperature, and humidity are monitored. Furthermore, inside one of the reactor segments, the temperature is monitored at different locations in the zeolite bed. Several tests, using different mass flow rates, have been performed. During the tests, a maximum temperature step of 24 ˚C was realized. The maximum delivered power was 4.4 kW and the obtained storage capacity was 52 kWh. The reactor efficiency was 76 % taking into consideration the conductive heat losses through the reactor wall and the sensible heat taken up by the thermal mass of the solids. Furthermore, it has been noticed that the flow through the bed was not completely uniform. This has a negative influence on the performance of the system.

Keywords: Thermochemical heat storage; open sorption system; segmented reactor; high power; zeolite 13X

Nomenclature

Roman letters	
A	Cross section area [m^2]
b	Isotherm model affinity constant [-]
c_p	Specific heat capacity at constant pressure [kJ/(kg · K)]
ΔE	Activation energy of desorption [J/mol]
h	Adsorption enthalpy [kJ/mol]
$LFDI$	Local velocity deviation index [-]
M	Molar mass [kg/mol]
$\dot{m}$	Mass flow rate [kg/s]
n	Isothermal model exponent constant [-]
P	Power [kW]
p	Pressure [Pa]
Q	Thermal energy [kJ]
q	Zeolite water loading [mol/kg]
R	Gas constant [J/(K · mol)]
t	Time [s]
T	Temperature [K]
U	Velocity [m/s]
V	Volume [m^3]
x	Absolute humidity [kg/kg]
Greek letters	
α	Isothermal model parameter
η	Efficiency [-]
ρ	Density [kg/m^3]
Subscripts	
eq	Equilibrium
rf	Reaction front
th	Theoretical

1 Introduction

Currently, the energy sector is undergoing a transition towards a more sustainable future. The use of fossil fuels is slowly phased out and more energy is produced by renewable energy sources. A promising renewable energy production technology is solar thermal, especially since heating accounts for 64% of the total energy consumption in Dutch households [1]. However, there is a seasonal mismatch between supply and demand regarding to solar thermal energy. During summer, solar energy is abundant but the demand for heating is low, while in winter the demand is high but the supply is low. This mismatch between supply and demand could potentially be resolved by seasonal thermal energy storage.

A promising method to store heat is by using sorption energy storage. This method allows for almost loss-free heat storage for a long time period [2, 3, 4]. The principle of sorption energy storage is based on a reversible interactions between the sorbate and sorbent according to $A(s) + B(g) \leftrightarrows AB(s) + heat$. During the endothermic charging process, heat is added to the sorption material, breaking the bonds of the sorbate to the sorbent, storing heat. At a later time, the stored heat can be retrieved by combining the sorbent and sorbate together (discharging). Here, the sorbent (A) is zeolite 13X and the sorbate (B) is water vapor. Zeolite is a good candidate to be used in reactor studies because of its high stability [5]. Since heat is not stored in a temperature difference between the material and the environment, but rather in the chemical bonds between sorbate and sorbent, there are no significant energy losses over long time periods.

In the past decade, lab or pilot setups have been developed and tested, attempting to integrate thermochemical heat storage in an overall system. Most of the systems utilize a packed-bed configuration. A disadvantage of the packed bed reactor design is the risk of formation of non-reactive zones, leading to a lower energy storage density. Table 1 shows open systems using zeolite as storage material.

Table 1: Open system prototypes along with operating conditions

Project name	Year	Material	T_{charge} [^oC]	$T_{discharge}$ [^oC]	Energy density [kWh/m^3]	Max Power [kW]
STAID [6]	2015	80 kg zeolite 13X	120-180	20	114	2.25
ASIC [7]	2014	50 kg zeolite 4A/X	230-180	25	148	1.5
E-HUB/ECN [8]	2014	150 kg zeolite 13X	185	25-60	58	0.4
PROMES-CNRS [9]	2014	400 kg $SrBr_2$	80	25	203	0.8
MONOSORP [10]	2006	70 kg zeolite 4A	170	20	120	1.5

Johannes et al. [6] realized a high power open sorption heat storage system (STAID), which contains two reactor segments, each containing 40kg of zeolite 13X. The system is to be integrated in a domestic ventilation system, and provide space heating during peak hours. The hydration temperature was kept at 20 ºC with a sorbate vapor pressure of approximately 16.3-15.8mbar. Running the segments in parallel, the system is able to supply a maximum thermal power output of 2.25 kW during 6 hours, with a maximum COP of 6.8. The power output is constant for 6 hours during the discharge phase. However, following this constant power period, the power output decreased during 4 hours to the point where the material is fully discharged. A maximum outlet temperature of 57 ºC was achieved.

In order to avoid the formation of non-reactive zones Zettl et al. [7] of the Austria Solar Innovation Center (ASIC) developed a rotating drum reactor filled with 50 kg zeolite 4A or zeolite X. This method is expensive and requires extra mechanical energy to revolve the reactor. At a hydration temperature of 25 ºC, the applied sorbate water vapor pressure was 25mbar. The system is able to deliver a maximum thermal power of 1.5 kW with a maximum COP of 12, taking into account the electrical power to operate the process. The maximum outlet temperature of the system is 60 ºC.

The E-HUB/ECN developed a prototype using two packed bed modules, totaling 150 kg zeolite 13X [8]. The aim is a compact long-term heat storage solution for low-energy single family houses. An air-to-air heat recovery unit was installed to increase the inlet temperature up to 40 ºC using residual heat in the outflow, which allows for higher outlet temperatures. The air flow to the zeolite bed is humidified to 12mbar water vapor pressure. The maximum delivered power is 0.4 kW, and the maximum outlet temperature of the system is 70 ºC.

The MONOSORP prototype is developed as an open heat storage system for space heating in the built environment [10]. The storage material is zeolite 13X and the system contains honeycomb structures instead of ordinarily employment fills. These structures have a large number of small straight channels that ensure a low pressure loss. The hydration temperature is approximately 20 ºC and the applied water vapor pressure is 12mbar. The maximum outlet temperature is approximately 42 ºC. The system delivers a maximum power output of 1.5 kW.

Michel et al. [9] developed a large scale prototype using 400kg of $SrBr_2$ packed in eight separate modules on top of each other. Each module has a reactive bed with a thickness of 7.5cm and a diffuser with a thickness of 1.5cm. In order to maximize the reactor energy storage density, the number of modules and diffusers should be minimized by using thicker reactive beds. However, a larger thickness limits mass transfer and reduces the thermal power output. This indicates that there is an optimum value in terms of reactive bed thickness. Gaeini et al. determined the optimal aspect ratio of the reactive bed [11]. This aspect ratio is implemented in the design of the pilot reactor of this work.

In this work, the design of a sorption storage system is presented, taking into account the issues reported in literature. The developed pilot reactor has several key characteristics to achieve a high-power, flexible system:

- The reactor segments have an optimum aspect ratio, which maximizes the efficiency and minimizes the pressure drop [11].
- The system is modular, which allows for easy upscaling.
- The segmented approach of the system reduces the pressure drop over the reactor vessels and decreases the sensible heat loss, therefore increasing the efficiency.
- The first reactor segment is equipped with additional thermocouples to investigate the formation of non-reactive zones.

The developed sorption energy storage system can be used to store heat for domestic applications. The main prospect of this technology is heat storage for domestic applications. It can provide temperatures suitable for space heating and with the addition of a heat recovery unit, temperature suitable for hot tap water. Experiments have been performed to demonstrate the power and capacity of the setup, and to investigate the non-reactive zones in the reactor bed. The developed pilot setup is in terms of energy density and sorption temperature is mapped in Figure 1, together with the previously described zeolite prototypes of Table 1.

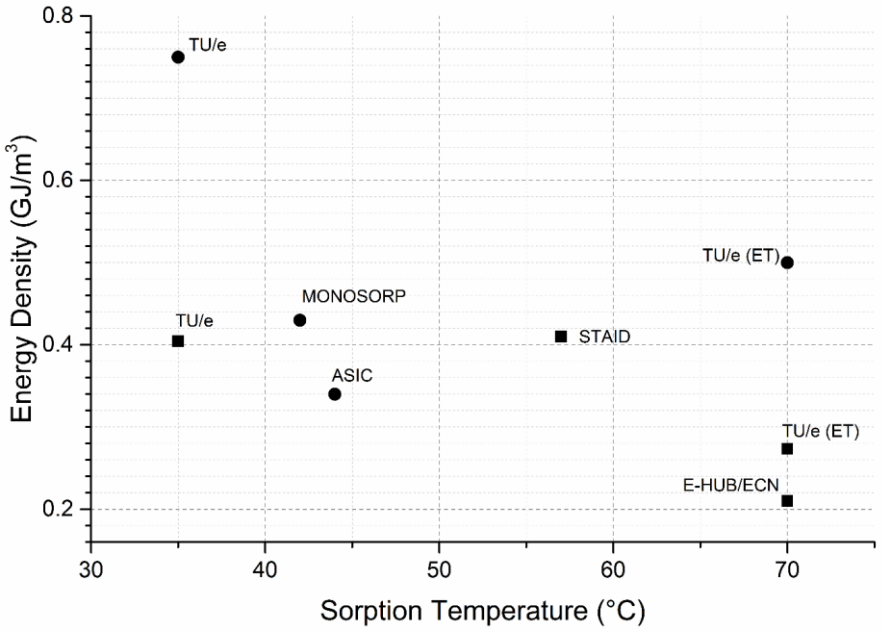

Figure 1: *Energy density vs sorption temperature of sorption heat storage prototypes based on zeolite with similar charging temperatures (~180 °C) and discharging water vapor pressure in the range 9 - 16 mbar. Square marker: energy density based on system/reactor volume. Circle marker: energy density based on material volume. TU/e: operating conditions reported in Table 2. TU/e (ET): operating conditions reported in Table 2 except for reactor inlet temperature, set at 50 °C.*

2 System analysis

A prototype setup is designed and built at the Eindhoven University of Technology. The setup is briefly explained here. More details can be found in [12]. Zeolite 13X (KÖSTROLITH) has been chosen as sorption material because of its high stability and relatively high energy storage density. More information on the material can be found in the detailed investigation done by Gaeini et al. [13].

2.1 Experimental setup

A segmented design has been selected for the system. This implies that there are a number of smaller separated compartments filled with zeolite. A segmented design has been selected because it has a number of advantages [14]:

- The pressure drop through the reactor will be reduced. Therefore, less fan power is required.
- Because the sorption material is divided over a number of reactors, only a part of the sorption material will be heated up when charging or discharging. This results in a faster response time and lower energy losses due to less sensible heat required to heat up the sorption material.
- It allows for easy scalability by increasing the number of segments.

The system consists of four reactor segments, each containing 62.5 liter of zeolite. All segments are identical, except for the first segment. This segment contains additional thermocouples, which allows monitoring of the temperature development inside the zeolite bed. The zeolite is placed between two perforated plates supported by a frame, to keep the grains in place. The inlet and outlet are placed on two opposite side walls, at the top and bottom of the reactor, respectively. The reactor design and sensor placement is displayed in Figure 2.

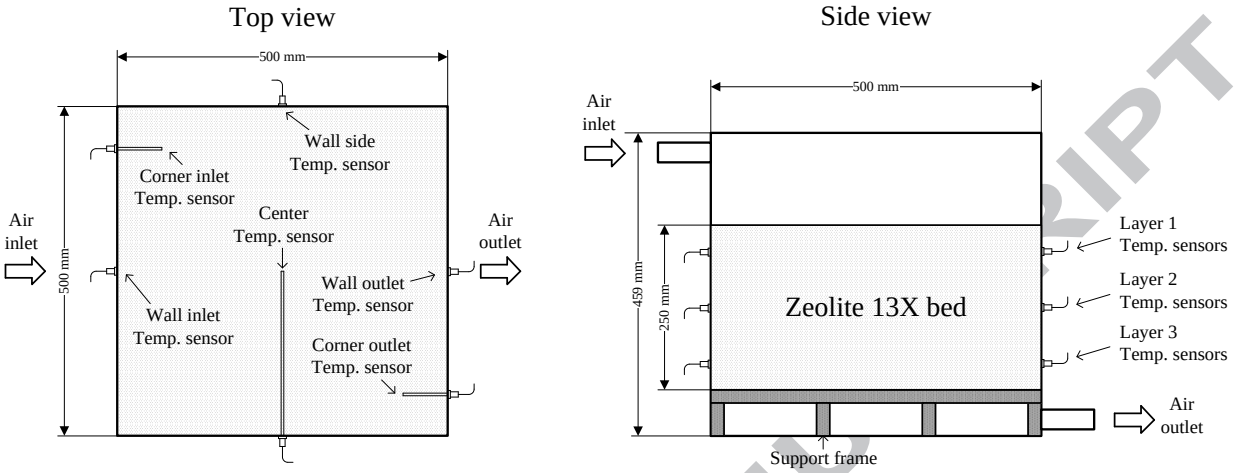

Figure 2: *Reactor design and sensor placement.*

In the setup, the air mass flow rate, humidity and air temperature are controlled. A schematic overview of the complete system is displayed in Figure 3. The air from a pressurized grid is fed to each segment with a controlled flow rate. After the mass flow controllers, 3-way valves have been installed in order to direct the air flow to the bubble columns for hydration, or to bypass the bubble columns for dehydration. The water level in the bubble columns are controlled to reach the desired humidity. After the bubble column in each path, another 3-way valve is placed to blow off the air flow during the stabilization period. The air passes through electric heaters, which simulate the solar thermal collectors. Then, the air passes through the reactors and is finally blown off to the environment. In each line, a number of sensors are placed, as shown in Figure 3. A picture of the setup is displayed in Figure 4.

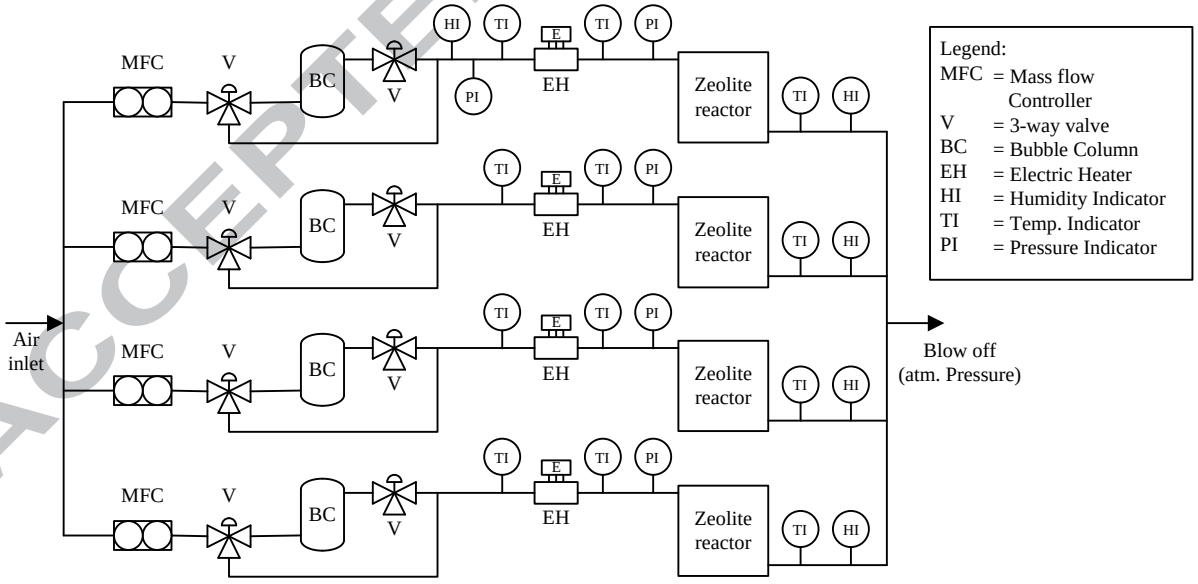

Figure 3: *Schematic overview of the experimental setup.*

Figure 4: *The setup without insulation.*

2.2 Experimental methodology

The operating conditions of the setup are displayed in Table 2.

Table 2: Typical operation parameters of experiments.

Parameter	Hydration	Dehydration	Unit
Inlet temperature	13	180	*[°C]*
Inlet vapor pressure	1348	85	*[Pa]*
Absolute humidity	10.2	0.41	*[g/m^3]*
Air mass flow rate	50	35	*[g/s]*

The theoretical energy storage capacity and thermal power of the setup can be calculated with Equations 1 and 2, respectively. Here, Δq_{eq} is the water uptake of zeolite 13X, which is determined using Langmuir-Freundlich equilibrium models and the inlet water vapor pressures during charging and discharging [13]. Δh_{avg} is the average adsorption enthalpy of zeolite 13X, which can be determined by using a mean value from the van 't Hoff equation [13]. V is the volume of the zeolite bed, ρ_{bulk} the bulk density of the zeolite, $\dot{m}$ the air mass flow rate, x the absolute humidity of the air and M_{water} the molar mass of water. This results in an energy storage capacity of 12.5 kWh and a thermal power of 1.6 kW per reactor segment.

$$Q_{th} = \Delta q_{eq}\, V\, \rho_{bulk}\, \Delta h_{avg} \tag{1}$$

$$P_{th} = \frac{\dot{m}_{air}\, x\, \Delta h_{avg}}{M_{water}} \tag{2}$$

The humidity at the inlet and outlet at one reactor segment is monitored. Therefore, the energy density can be calculated based on the experimentally obtained water uptake. However, temperature sensors are also placed in the setup allowing the energy storage capacity to be calculated based on the temperature. The advantage of calculating the energy storage capacity based on the inlet and outlet temperatures compared with the calculating it based on the inlet and outlet humidity is that the latter does not require an assumption for the average adsorption enthalpy. Therefore, the extracted energy from a segment while discharging has been calculated with Equation 3. Herein, c_p is the specific heat capacity of air and t_0 and t_e are the start and the end time, respectively.

$$Q_{discharging} = \dot{m}_{air}\, c_{p,air} \int_{t_0}^{t_e} |T_{out}(t) - T_{in}(t)|\, dt \tag{3}$$

The same equation can be used to calculate the introduced energy into the segment during charging ($Q_{charging}$). The efficiency of the system is calculated with Equation 4 [15]. Here, $Q_{charging}$ is the energy required to dehydrate the reactor segments. The air fed to the system comes from a pressurized grid. Therefore, the required fan power in an actual

system has not been included in the efficiency. It also should be noticed that the thermal energy that is blown off through the outlet when charging is not considered as a loss in the calculation. This is because the energy can (partly) be used for the pre-heating of a segment or sensible heat storage. Finally, despite the storage of energy being loss-free, there are some losses during the charging and discharging of the reactor. When the reactor is discharged, a temperature difference between reactor and ambient is created causing heat losses to the surroundings.

$$\eta = \frac{Q_{discharging}}{Q_{charging}} \tag{4}$$

In order to determine if the reactor performs optimally, it needs to be determined if the zeolite bed is charged and discharged uniformly. The flow uniformity index is introduced to evaluate this aspect [16, 17] and is displayed by Equation 5. Herein, U_{rf} is the experimentally obtained local reaction front velocity based on temperature measurements. $U_{rf,avg}$ is the average reaction front velocity, which can be calculated with Equation 6. The flow uniformity index can be obtained when the flow velocity over the whole cross section area of the bed is known. In the experimental setup, the flow is investigated at six different points per layer as shown in Figure 2. Therefore, the local velocity deviation index is used to define the uniformity of the flow at these six points.

$$LFDI = \frac{U_{rf} - U_{rf,avg}}{U_{rf,avg}} \tag{5}$$

The local front velocity U_{rf} is not obtained directly, but estimated at the thermocouple location by calculating the time between the beginning of the experiment and the time at which the thermocouple temperature started to decrease, indicating that the reaction front passed that location of the bed. The average velocity $U_{rf,avg}$, at which the reaction front is traveling through the bed, has been calculated based on Equation 6. Herein, A is the cross section surface of the zeolite bed.

$$U_{rf,avg} = 1 - \frac{\dot{m}\, x}{A\, \rho_{bulk}\, q\, M_{water}} \tag{6}$$

3 Results

In this section, experimentally obtained results are presented and discussed. First, the general performance of the prototype setup is demonstrated based on the energy storage capacity and thermal power output. Then, the importance of partial discharging of the reactor segments are evaluated. Furthermore, the flow uniformity as an effective factor on the performance of the system, is investigated.

3.1 Energy storage capacity and thermal power demonstration

To demonstrate the energy storage capacity and power of the system, all four segments have been discharged multiple times at different air mass flow rates. The temperatures at the inlets and outlets of all the segments have been monitored. The results of the experiment with an air mass flow rate of 50 g/s per segment are shown in Figure 5.

The energy that is extracted from a segment while discharging, is calculated with Equation 3. The time interval that is used to calculate the extracted energy is 18 hours, based on the time it takes to discharge a segment at an air flow rate of 50g/s. The results of this calculation are shown in Figure 6. Figure 6 also includes the thermal power of the segments. To calculate the power, the temperature step at which the system was running steadily has been used. The system has been considered steady between 4 and 9 hours, in Figure 5.

The expected theoretical energy storage capacity of the reactor segments is 12.5 kWh, based on the energy density of zeolite. From the results in Figure 6, it can be observed that the recovered energy from a reactor segment varies between 12.5 and 14 kWh, with an average capacity of 13 kWh. Especially the first segment performs better than expected. This is because the zeolite has been replaced in this reactor, which probably improved the packing of the material, and hence increased its bulk density.

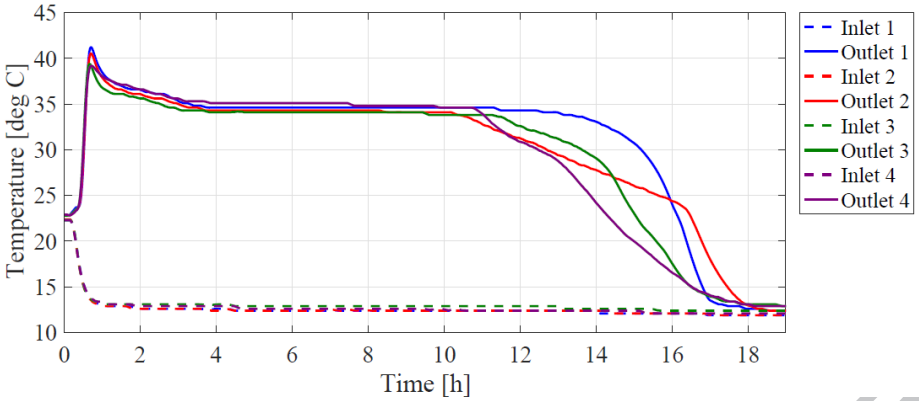

Figure 5: *Inlet and outlet temperatures per segment while discharging at 50 g/s.*

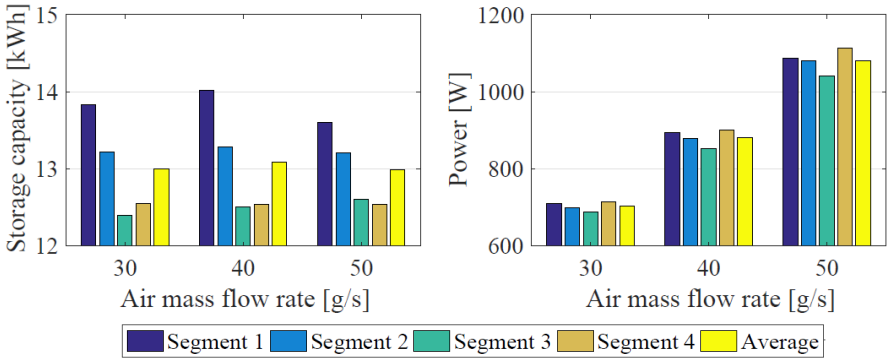

Figure 6: *Energy storages capacities and delivered powers per segment.*

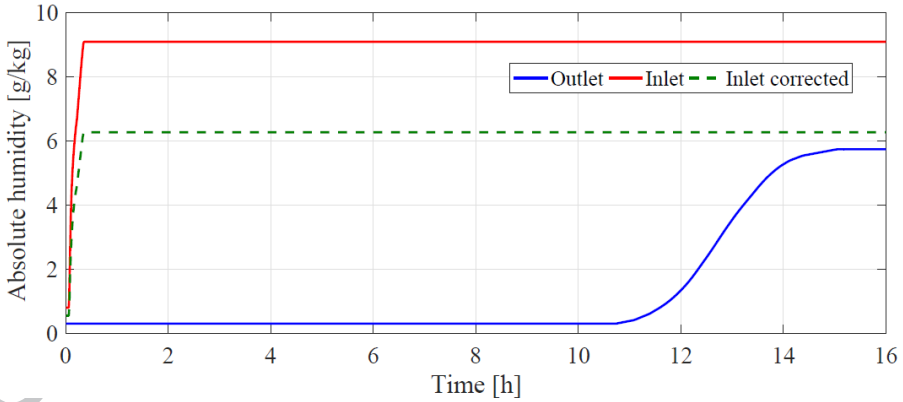

Figure 7: *Absolute humidity at the inlet and outlet of segment one while discharging at 50 g/s.*

The expected power of a reactor segment has been calculated with Equation 2. This resulted in an expected power of 1.55 kW per reactor segment at an air mass flow rate of 50 g/s. However, the experimentally obtained power is 1.1 kWh, as can be observed in Figure 6. This difference is caused by a lower humidity produced in the bubble columns compared to the expected one. There is an overpressure in the humidifiers due to the pressure drop over the components after the bubble columns (Figure 2). In the humidifiers, the air is humidified to a certain vapor pressure, which is not a function of the total pressure. Therefore, x (in kg water/kg air) is lower than if ambient pressure air would have been used, resulting in lower thermal power in accordance with equation 2. In Figure 7, the humidity at the inlet and outlet of a reactor segment is shown. It can be seen that the inlet and outlet humidity do not reach the same value. This is because the sensors do not correct for the total pressure. Therefore, a pressure sensor has been installed near the humidifier to correct the humidity by dividing it to the total pressure, which is also shown in Figure 7. When this correction is included in the theoretical power calculation, a power of 1.1 kW is obtained for an air mass flow rate of 50 g/s, which is the same as the experimentally obtained power.

The temperature development during dehydration of the zeolite reactors is displayed in Figure 8. It can be observed that water is released at certain temperatures, since the temperature at the outlets does not increase with the same trend as at the inlets. The average energy fed to each segment for dehydration is 17 kWh. Therefore, 4 kWh more energy is fed to the reactor during dehydration (charging) than what is recovered during hydration (discharging). There are two main reasons for this. First, there is approximately 2.5 kWh of sensible heat required to heat up the reactor and the sorption

material to 180˚C. Then, there are losses to the environment due to temperature differences. However, a relatively high efficiency of 76.4 % is calculated for this system. When the sensible heat of the reactor and sorption material can be used, the efficiency can be increased up to 91.2 %. Furthermore, it can be noticed that the difference between the inlet and outlet temperature is about 10˚C when the reactors are fully charged, which is probably due to losses.

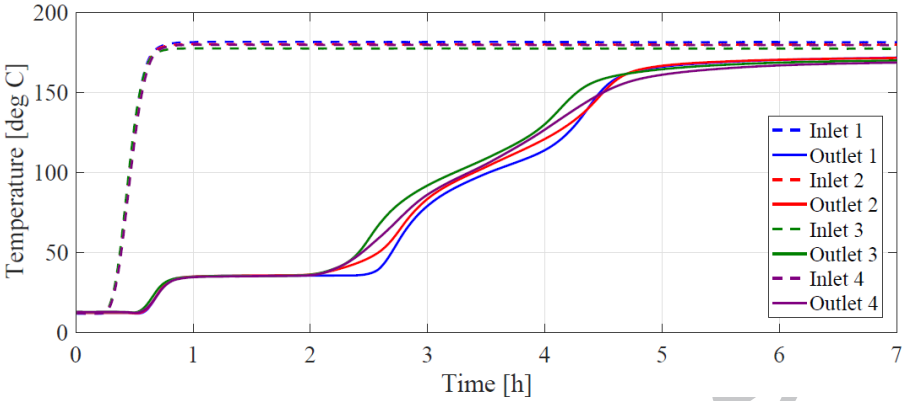

Figure 8: *Inlet and outlet temperatures per segment when charging at 35 g/s and 180˚C.*

In order to estimate the reactor energy density with a sorption temperature suitable for domestic hot water production, the reactor inlet temperature has been increased from 10 °C to 55 °C by preheating the inlet air with the heaters (Figure 2). An outlet temperature of approximately 75 °C has been reached. The airflow rate during this experiment was 30 g/s and the discharging time was in the order of 18 hours, with the outlet temperature starting to decrease after approximately 14 hours from the beginning of the discharge. The average energy content per segment was 8.8 kWh, which resulted in an energy density of approximately 0.49 and 0.29 GJ/m^3.

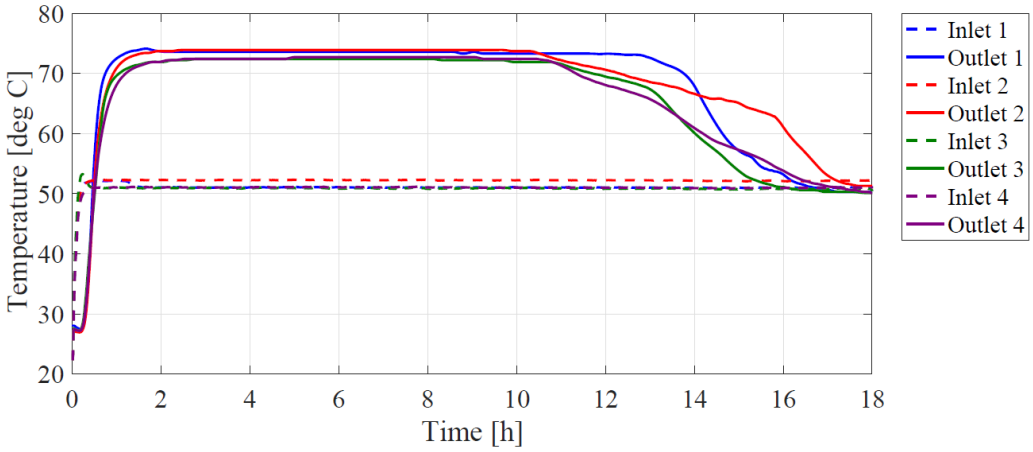

Figure 9: *Bed temperature profiles during a discharging experiment with a reactor inlet temperature of 55 °C and an airflow rate of 30 g/s. [18]*

3.2 Partial discharge of segments

In practice, a segment can be partially discharged if, for example, not all its energy content is required by the thermal load. In that case, water might diffuse from the hydrated to the dehydrated part of the bed. This will result in energy losses because the first water molecules adsorbed by the zeolite contain more energy than the last adsorbed molecules. Therefore, the effects of diffusion have been investigated. This has been done by discharging a reactor segment in two separated periods, with a shutdown period among the two partial discharge periods.

The temperature development in the middle layer of the bed of an experiment with a waiting time of 23 hour has been included in Figure 10. From the left graph, it can be observed that the bed has been fully hydrated at 4 of the 6 locations, before the air mass flow rate was stopped. In the right graph, the second discharging stage can be observed. It can be observed that there is a temperature increase of approximately 4˚C at the locations where the bed was supposedly already hydrated. This might be caused by water diffusion. However, to be more certain, another experiment with a longer waiting period has been performed. The temperature development of this experiment has been included in Figure 11.

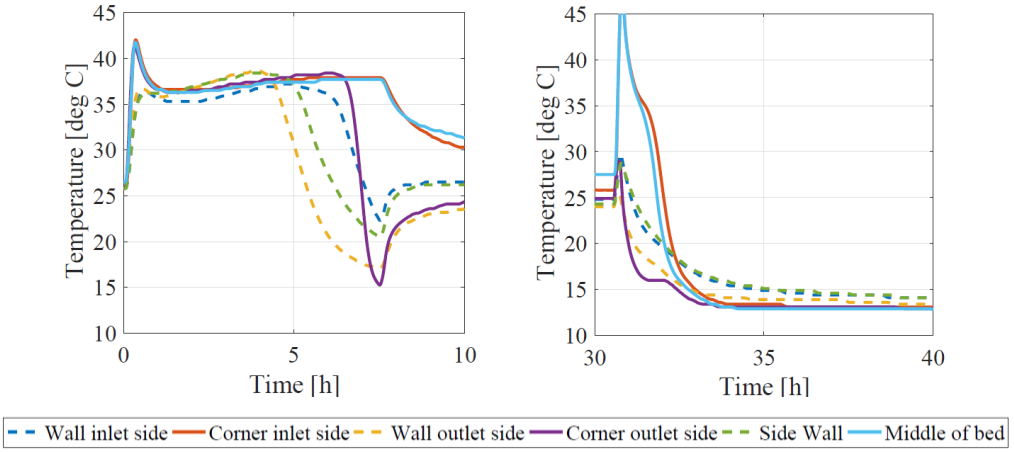

Figure 10: *Temperature development at the in- and outlets of the reactor segments when discharging at 40 g/s in two consecutive periods with approximately 1 day in between.*

From Figure 11, it can be observed that the first discharging stage is similar to the results presented in Figure 10. However, in the second discharging stage, the temperature increase at the hydrated part of the bed is approximately 8˚C. This indicates that more water has been diffused away from this hydrated region. However, the energy storage capacity did decrease by 1.5 % in the experiment presented in Figure 10, while it only did decrease by 1.2 % in the experiment presented in Figure 11. Therefore, it can be concluded that diffusion within this type of material, at these operating conditions, is a slow process, and it does not have a significant effect on the energy storage capacity of the present setup.

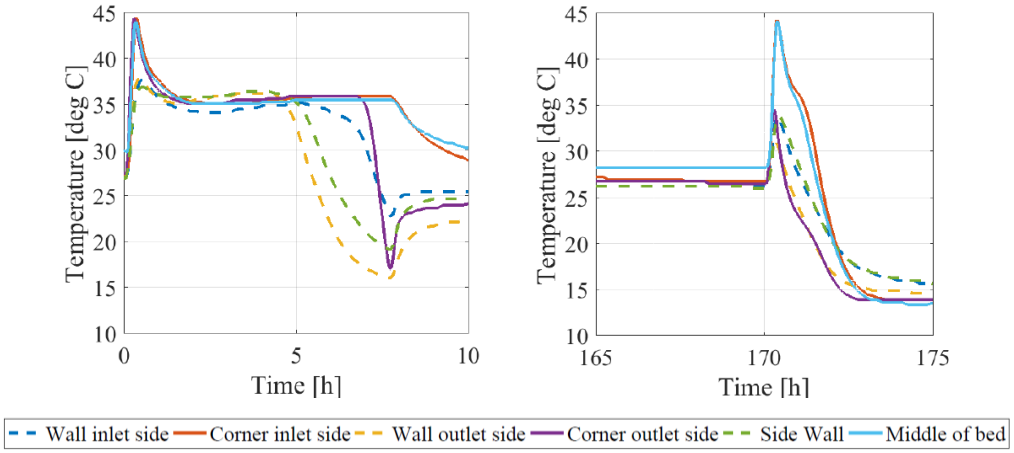

Figure 11: *Temperature development at the inlets and outlets of the reactor segments when discharging at 40 g/s in two consecutive periods with approximately 7 days in between.*

3.3 Flow uniformity

Flow uniformity defines the flow velocity distribution through a cross section of the zeolite bed. A high flow uniformity is important for the system to work as efficiently as possible. Therefore, the flow uniformity has been investigated experimentally by considering the temperature development in the reactor bed.

In Figure 12, the temperature development inside the zeolite bed are shown. In these graphs, the vertical black dashed lines indicate the times at which the bed is expected to be hydrated (with perfect flow uniformity), which have been calculated with Equation 6. From Figure 12a, it can be observed that the calculated time corresponds relatively well with the experimentally obtained time. Furthermore, it can be observed from figure 12b-d that the flow through the bed is not completely uniform based on the temperatures in the bed. For instance, at the middle layer of the bed (figure 12c), the zeolite at the outlet side wall is discharging about twice as fast as the middle of the bed at the same height. Because of this, the outlet temperature of the reactor starts to decrease while other parts of the zeolite are still discharging.

Figure 13 shows the local flow deviation index (LFDI) explained in section 2.4. The LFDI is determined with an air mass flow rate of 50g/s per segment. In Figure 13, the colored bars are the results of an experiment after replacing the zeolite and the gray bars are the results before the zeolite has been replaced. It can be observed that the differences between these experiments are large. Therefore, the packing of the zeolite has a big impact on the flow distribution through the bed. However, some trends are visible. The highest reaction front velocities can be expected near the walls, due to the higher porosity at the wall regions [11, 19, 20]. This was also observed while performing the experiments.

The overall highest velocity was observed at the outlet wall. This is because the air is blown into the reactor with a relatively high velocity, and the inlet is directed at the outlet wall. This directs the flow directly into the bed at the outlet wall side. The lowest velocity is observed in the middle of the bed.

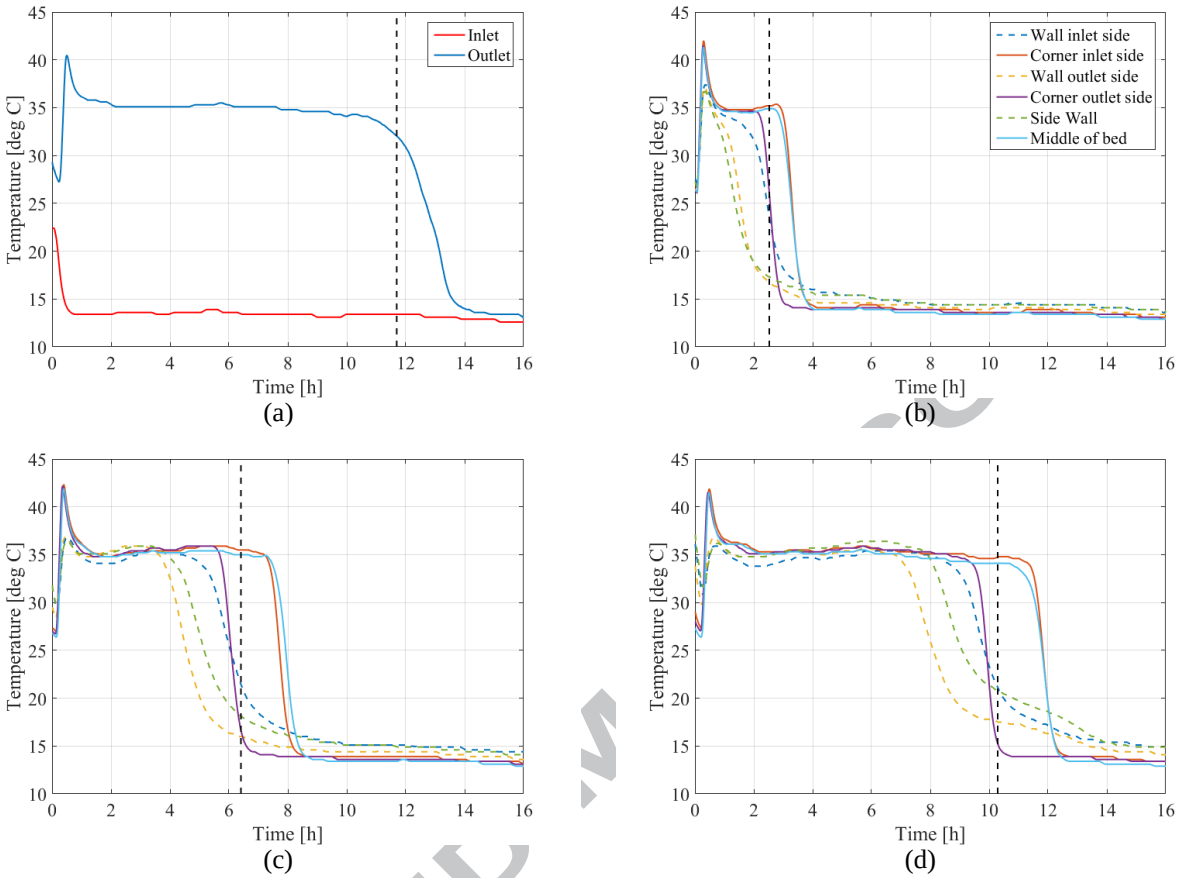

Figure 12: *Temperatures development at various locations in the bed while discharging at an air mass flow rate of 50 g/s per segment. (a) inlet and outlet temperature, (b) temperature on the top layer, (c) temperature on the middle layer and (d) temperature on the lowest layer. The vertical dashed lines are expected discharge times.*

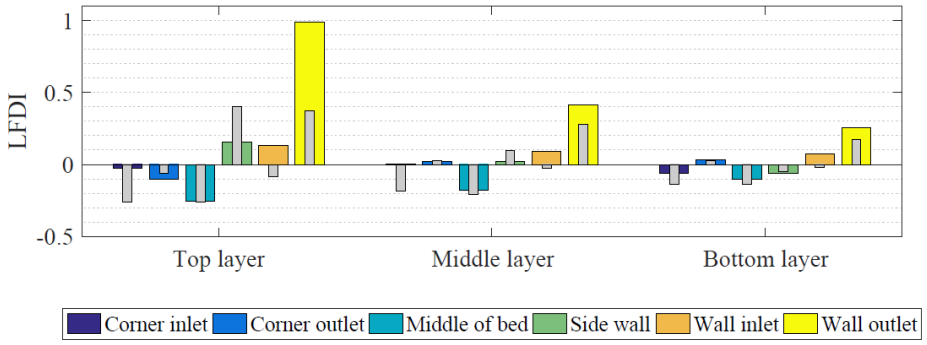

Figure 13: *Local velocity deviation indexes when discharging at 50 g/s per segment: the colored bars are the results from an experiment after replacing the zeolite and the gray bars are the results from an experiment before the zeolite replacement and repacking of the bed.*

The average of the absolute values of the velocity deviation indexes for different location of temperature sensors and different flow rates are displayed in Table 3. It can be observed that mass flow rate, and thus the pressure drop over the bed, has an effect on the uniformity of the flow. In general, the flow uniformity increases when the mass flow decreases. It can be noticed that the velocity deviation indexes are higher at the top thermocouple layer than at the other two layers. This is probably due to the effect of the inlet turbulent airflow. While advancing through the porous bed, the airflow increases its uniformity.

Table 3: Absolute average velocity deviation indexes per layer at 30, 40 and 50 g/s air mass flow.

Parameter	Top layer	Middle layer	Bottom layer	Average
50 g/s	0.241	0.137	0.091	0.156
40 g/s	0.225	0.128	0.084	0.146
30 g/s	0.208	0.121	0.085	0.138

4 Conclusions and outlook

In this paper, the development of a zeolite 13X/water sorption storage system has been described. The system has been developed to investigate the possibilities of a large scale seasonal sorption thermal energy storage for households. The setup consists of four separate segments with 62.5 liter zeolite each.

With the setup, a number of experiments have been performed. From the results in this paper, it can be concluded that the setup storage efficiency is 76 % and that it can be increased to 91 % if the sensible heat of the solid materials of the reactor can be recovered. However, the energy that is blown of through the outlet when charging was not considered as a loss in the calculation because it could still be usable. The setup is able to store about 54 kWh thermal energy and can deliver powers of 4.4 kW. The power is lower than expected, which is caused by a lower air humidity *x*, caused in turn by a high pressure in the humidifier. Therefore, minimizing the pressure drop in the system improves also the thermal performance of the system.

An experiment with an elevated inlet temperature of 55 °C has been performed with an air flow rate of 30 g/s. An energy density of 0.49 GJ/m^3 referred to the material volume has been measured with a sorption temperature of approximately 75 °C. This latter result opens opportunities for domestic hot water production with this reactor prototype, assuming that a heat recovery system is integrated.

Diffusion of water inside a partially hydrated zeolite bed has also been investigated experimentally. From these results, it can be concluded that local diffusion does occur, but that it is a very slow process. Therefore, diffusion does not have a significant effect on the energy storage capacity of the reactor segments.

Furthermore, the uniformity of the flow through the zeolite bed has been investigated, since flow uniformity is important to have a constant power during the discharging time and to make a complete system work as efficiently as possible. From the performed experiments, it is observed that the flow uniformity is not ideal and that the distribution of the zeolite grains has a big effect on the flow distribution.

Acknowledgements

This research has been made possible by the Smart Energy Regions Brabant program, funded by the Dutch province of North-Brabant.

References

1. Energietrends 2016. ECN, Energie-Nederlands and Netbeheer Nederland, 2016.
2. Aydin, D., Casey, S. P., & Riffat, S. (2015). The latest advancements on thermochemical heat storage systems. Renewable and Sustainable Energy Reviews, 41, 356-367.
3. Tatsidjodoung, P., Le Pierrès, N., Heintz, J., Lagre, D., Luo, L., & Durier, F. (2016). Experimental and numerical investigations of a zeolite 13X/water reactor for solar heat storage in buildings. Energy Conversion and Management, 108, 488-500.
4. N'tsoukpoe, K. E., Liu, H., Le Pierrès, N., & Luo, L. (2009). A review on long-term sorption solar energy storage. Renewable and Sustainable Energy Reviews, 13(9), 2385-2396.
5. Jänchen, J., Schumann, K., Thrun, E., Brandt, A., Unger, B., Hellwig, U. (2012). Preparation, hydrothermal stability and thermal adsorption storage properties of binderless zeolite beads, Int. J. Low-Carbon Technol. 7 (4) 275–279.
6. Johannes, K., Kuznik, F., Hubert, J. L., Durier, F., & Obrecht, C. (2015). Design and characterisation of a high powered energy dense zeolite thermal energy storage system for buildings. Applied Energy, 159, 80-86.
7. Zettl, B., Englmair, G., Steinmaurer, G. (2014). Development of a revolving drum reactor for open-sorption heat storage processes, Applied Thermal Engineering 70 (1), 42 – 49.
8. de Boer, R., Smeding, S., Zondag, H. A., & Krol, G. (2014, May). Development of a prototype system for seasonal solar heat storage using an open sorption process. In Eurotherm Seminar# 99, Advances in Thermal Energy Storage 28-30.
9. Michel, B., Mazet, N., Neveu, P. (2014). Experimental investigation of an innovative thermochemical process operating with a hydrate salt and moist air for thermal storage of solar energy: Global performance, Applied Energy 129, 177 -186
10. Bales, C., Gantenbein, P., Jaenig, D., Kerskes, H., Summer, K., van Essen, M., & Weber, R. (2008). Laboratory tests of chemical reactions and prototype sorption storage units. A Report of IEA Solar Heating and Cooling programme-Task, 32.
11. Gaeini, M., Wind, R, Donkers, P.A.J., Zondag, H.A., Rindt, C.C.M. (2017). Development of a validated 2D model for flow, moisture and heat transport in a packed bed reactor using MRI experiment and a lab-scale reactor setup, International Journal of Heat and Mass Transfer, 113, 1116-1129.
12. Gaeini, M., Javed, M.R., Ouwerkerk, H., Zondag, H.A. & Rindt, C.C.M. (2017). Realization of a 4kW thermochemical segmented reactor in household scale for seasonal heat storage. Energy Procedia, 135, 105-114.

13. Gaeini, M., Zondag, H.A., Rindt, C.C.M. (2016). Effect of kinetics on the thermal performance of a sorption heat storage reactor, Applied Thermal Engineering 102, 520-531.
14. Weber, R., Asenbeck, S., Kerskes, H., & Drück, H. (2016). SolSpaces–Testing and Performance Analysis of a Segmented Sorption Store for Solar Thermal Space Heating. Energy Procedia, 91, 250-258.
15. Abedin, A. H., & Rosen, M. A. (2012). Closed and open thermochemical energy storage: energy-and exergy-based comparisons. Energy, 41(1), 83-92.
16. Guhan, C. O. A., Arthanareeswaran, G., Varadarajan, K. N., & Krishnan, S. (2016). Numerical optimization of flow uniformity inside an under body-oval substrate to improve emissions of IC engines. Journal of Computational Design and Engineering, 3(3), 198-214.
17. Zhang, X., Gomulka, T., & Romzek, M. (2007). Numerical optimization of flow uniformity inside an F-oval substrate (No. 2007-01-1088). SAE Technical Paper.
18. Gaeini, M., van Alebeek, R., Scapino, L., Zondag, H.A., Rindt, C.C.M. (2018). Hot tap water production by a 4kW sorption segmented reactor in household scale for seasonal heat storage. Journal of Energy Storage, 19, 118-128.
19. Atmakidis, T., & Kenig, E. Y. (2009). CFD-based analysis of the wall effect on the pressure drop in packed beds with moderate tube/particle diameter ratios in the laminar flow regime. Chemical Engineering Journal, 155(1), 404-410.
20. Chandrasekhara, B. C., & Vortmeyer, D. (1979). Flow model for velocity distribution in fixed porous beds under isothermal conditions. Wärme-und Stoffübertragung, 12(2), 105-111.